

# Synthesis and microwave properties of $\text{Tl}_2\text{Ba}_2\text{CaCu}_2\text{O}_8$ superconducting films grown by MOCVD

G. Pica<sup>1,a</sup>, A. Andreone<sup>1</sup>, F. Palomba<sup>1</sup>, M. Salluzzo<sup>1</sup>, R. Vaglio<sup>1</sup>, G. Malandrino<sup>2</sup>, V. Ancarani<sup>2</sup>, I.L. Fragalà<sup>2</sup>, A. Cassinese<sup>3,b</sup>, and G. Müller<sup>3</sup>

<sup>1</sup> I.N.F.M and Dipartimento di Scienze Fisiche, Università' di Napoli Federico II, Napoli, Italy

<sup>2</sup> Dipartimento di Scienze Chimiche and I.N.S.T.M., Università' di Catania, Catania, Italy

<sup>3</sup> Fachbereich Physik, Bergische Universität Wuppertal, Wuppertal, Germany

Received 16 December 1999 and Received in final form 17 March 2000

**Abstract.** We report on the synthesis, structural and electrical characterization of high quality  $\text{Tl}_2\text{Ba}_2\text{Ca}_1\text{Cu}_2\text{O}_8$  (Tl-2212) superconducting films. The samples have been grown *ex-situ* on  $10 \times 10 \text{ mm}^2$   $\text{LaAlO}_3$  (100) substrates by a combined approach of metal-organic chemical vapor deposition (MOCVD) and thallium vapor diffusion. The morphological and compositional nature of the *c*-axis oriented films has been investigated by SEM and X-ray analyses. Typical values of  $T_c = 104 \text{ K}$  and  $J_c = 0.5 \text{ MA/cm}^2$  at  $77 \text{ K}$  have been measured. Microwave measurements have been performed at  $f = 87 \text{ GHz}$  inserting the film in a copper cavity and at  $f = 1.5 \text{ GHz}$  on patterned samples using a microstrip resonator technique. A penetration depth  $\lambda(0) = 400 \text{ nm}$  is evaluated by fitting the microwave data with phenomenological equations. The minimum value of the surface resistance  $R_s$  measured at  $4.2 \text{ K}$  is  $60 \mu\Omega$  and  $6 \text{ m}\Omega$  at  $1.5 \text{ GHz}$  and  $87 \text{ GHz}$  respectively. The microwave data are described in the context of a modified two fluid model. An evaluation of the temperature dependence of the scattering rate has been performed through the simultaneous measurement of the surface resistance and the penetration depth.

**PACS.** 74.25.Nf Response to electromagnetic fields (nuclear magnetic resonance, surface impedance, etc.) – 74.20.De Phenomenological theories (two-fluid, Ginzburg-Landau, etc.) – 74.72.Fq Tl-based cuprates

## Introduction

Over the past years there has been an increasing interest in the properties of  $\text{Tl}_2\text{Ba}_2\text{Ca}_1\text{Cu}_2\text{O}_8$  (Tl-2212) and  $\text{Tl}_2\text{Ba}_2\text{Ca}_2\text{Cu}_3\text{O}_{10}$  (Tl-2223) superconducting films because of their higher  $T_c$  values compared to the more popular  $\text{YBa}_2\text{Cu}_3\text{O}_{7-\delta}$  (YBCO) compound. In particular, the insertion of Tl-based films in electronics allows for devices operating at lower reduced temperatures where the superconducting properties are better established [1] or, alternatively, the use of simpler and lighter cooling systems working at higher temperatures without compromising device performance. In respect to the potential application, Tl-2212 is characterized by greater ease of preparation, even if the optimum  $T_c$  (110 K) is slightly lower, compared to Tl-2223 ( $T_c = 125 \text{ K}$ ). Specifically, Tl-2212 presents a lower formation temperature which prevents chemical reaction with the substrate, resulting in better growth conditions on buffer layered substrates or in the case of double-sided films [2]. In this work we report on the

synthesis and microwave characterization of Tl-2212 films grown by a combined approach of metal-organic chemical vapor deposition (MOCVD) and thallium vapor diffusion. Tl-2212 films have been previously grown by a two step post-annealing process using laser ablation [3], magnetron [2] or off-axis sputtering [4,5]. MOCVD has the potential advantage of being a very reliable and reproducible technique for the fast production of films with a high degree of uniformity over large areas for both thickness and composition.

Microwave study can be an important tool in establishing the nature of cuprate electrostatics, and measurements of both surface resistance and penetration depth and of their correlation with material properties are highly desirable. However, while the behavior of surface impedance  $Z_s$  has been widely investigated for YBCO single crystals and films [6], only little work exists on the intrinsic microwave properties of Tl-based compounds. In this context, some papers have been published on the overdoped cuprate  $\text{Tl}_2\text{Ba}_2\text{CuO}_{6+\delta}$  (Tl-2201) because of its very simple tetragonal crystal structure, with a single  $\text{CuO}_2$  plane/unit cell. Recently, Broun *et al.* [7] reported a linear dependence of  $\lambda(T)$  at low temperatures in Tl-2201 single crystals, suggesting an unconventional pairing state

<sup>a</sup> e-mail: pica@na.infn.it

<sup>b</sup> Present address: I.N.F.M. and Dipartimento di Scienze Fisiche, Università' di Napoli Federico II, Napoli, Italy

with line nodes that closely resembles what observed in  $\text{YBa}_2\text{Cu}_3\text{O}_{7-\delta}$  and  $\text{Bi}_2\text{Sr}_2\text{CaCu}_2\text{O}_8$ . Microwave measurements of the real part of the in-plane conductivity showed a broad, frequency dependent peak near 30 K similar to what found in other cuprates. This result has been interpreted as due to a rapid decrease in scattering of thermally activated quasiparticles on entering the superconducting state [8]. Similar measurements have been reported by Huber *et al.* [9] in high quality Tl-2223 films using a cavity technique at 87 GHz. An unusual behaviour, which the authors state to be consistent with a *d*-wave scenario, has been also described by Willemsen *et al.* [10] investigating in high quality Tl-2212 films intermodulation signals as a function of the input power. However, other origins of nonlinearity, such as weak links, can also account for the observed dependence.

We report here a study of the temperature dependence of the surface resistance, penetration depth and quasiparticle scattering time in selected Tl-2212 films grown by MOCVD. Specifically, in Section 2 the details of the deposition process, and the structural and transport properties of the superconducting films are reported. The microwave response measured on as-grown and patterned samples is the subject of Section 3. Two different techniques, a microstrip resonator at  $f = 1.5$  GHz and a copper cavity at  $f = 87$  GHz, are employed for the measurement of the electrodynamic properties. Finally, in Section 4 the microwave data of the best Tl-2212 films are reported and described in the framework of a modified two fluid model with comparison with high quality YBCO films. In particular, the temperature dependence of the quasiparticle scattering time  $\tau$  is evaluated without any assumption on the value of  $\lambda(0)$ .

## Film deposition, structural and transport properties

Tl-2212 films have been grown on  $\text{LaAlO}_3$  (100) oriented  $10 \times 10 \times 0.5$  mm<sup>3</sup> substrates through a classical *ex-situ* two step process:

- synthesis of BaCaCuOF matrices by MOCVD;
- thallium vapor diffusion.

The BaCaCuOF matrices have been deposited from Ba(hfa)<sub>2</sub>-tetraglyme, Ca(hfa)<sub>2</sub>-tetraglyme (Hhfa = 1,1,1,5,5,5-hexafluoro-2,4-pentanedione, tetraglyme = 2,5,8,11,14-pentaoxatetradecane) [11] and Cu(acac)<sub>2</sub> (Hacac = acetylacetone) precursors in a low pressure, horizontal, cold wall reactor with a resistive substrate heater. Particular attention has been devoted to the optimization of the sublimation temperatures of the precursors to obtain the correct stoichiometry of the matrix. Energy dispersive X-ray (EDX) analyses of several selected areas ( $100 \times 100$  μm<sup>2</sup>) indicate that the  $2 \pm 0.2 : 1 \pm 0.1 : 2 \pm 0.2$  stoichiometry is found over the whole  $10 \times 10$  mm<sup>2</sup> surface. In addition, the run to run reproducibility is very good with high yield (> 80%) of Ba-Ca-Cu matrices having the right composition.

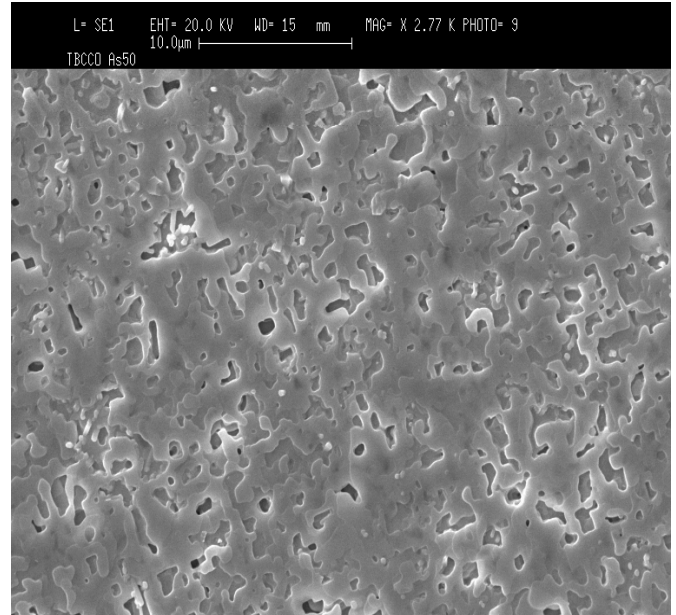


**Fig. 1.** SEM image of the surface of a Tl-2212 film grown on a  $10 \times 10$  mm<sup>2</sup>  $\text{LaAlO}_3$  (100) substrate.

An open reactor has been used for the thallium vapor diffusion step. The as-deposited films containing fluoride phases are directly annealed in a gold covered crucible. The thallium vapor pressure is provided by the  $\text{Tl}_2\text{O}_3$  present in the mixed powder of oxides having the following stoichiometry:  $1\text{Tl}_2\text{O}_3 : 1\text{BaO} : 2\text{CaO} : 3\text{CuO}$ . The reaction atmosphere is controlled by mixing different flows of oxygen and argon gasses. Preliminary data on the correlation of oxygen partial pressure and temperature [12] on the formation of Tl-Ba-Ca-Cu-O phases clearly indicate that lower oxygen partial pressure requires lower annealing temperatures [13]. The present films were annealed at a temperature of 820 °C for 40 min using an oxygen partial pressure of  $0.7 \times 10^5$  Pa. The thickness of the films after the thallium vapor diffusion step was between 1 and 1.3 μm. The stoichiometry after the thalliation process is  $2 \pm 0.2 : 2 \pm 0.2 : 1 \pm 0.1 : 2 \pm 0.2$  over the whole  $10 \times 10$  mm<sup>2</sup> surface. Therefore, the observed stoichiometries point to a good reproducibility in terms of composition both in regard to the MOCVD deposition as well as to the annealing process.

This last one represents the crucial step to produce high-quality Tl-2212 films. In particular, the gold covered crucible is promising for the fabrication of double-sided films for device applications. Preliminary results indicate that the presently used geometry is a powerful tool to grow high quality Tl-based films on both sides of the substrate [14].

The Scanning Electron Microscopy (SEM) images show that the surface is very smooth with well interconnected grains of average diameter of 10–15 μm (see Fig. 1). Pinholes are usually present on the film surface while outgrowths are observed only when a slight different stoichiometry is observed for Ba or Cu elements. The X-Ray Diffraction (XRD) data of these samples indicate

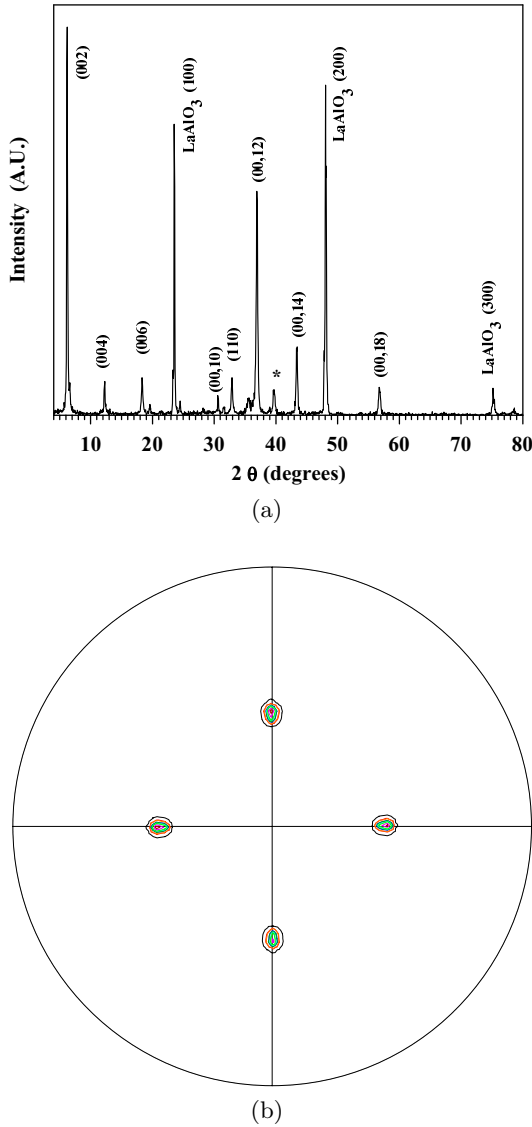


**Fig. 2.** (a) XRD pattern and (b) (107) pole figure of a Tl-2212 film.

that the films are highly  $c$ -axis oriented and monophasic. In fact, the XRD pattern (Fig. 2a) primarily shows the presence of the (001) reflections of the Tl-2212. In addition, a small peak has been observed that can be indexed as the Tl-2212 (110) reflection. The peak at  $39.70^\circ$  could not be indexed. To gain further insight into the in-plane crystallography, the pole figure of the Tl-2212 (107) reflection ( $2\theta = 31.45^\circ$ ) has been collected using a 4-circle goniometer. In this polar plot, shown in Figure 2b, the radial dimension  $\chi$  is the angle between the normal of the film surface and the plane of the X-ray beam. The azimuth,  $\Phi$ , corresponds to the rotation of the substrate about the surface normal. The pole figure shows that the TBCCO film is epitaxially grown on the  $\text{LaAlO}_3$  (100) substrate. In fact, four reflections at  $\chi = 47.8^\circ$  are observed every  $90^\circ$  of  $\Phi$  as expected for this tetragonal material.

The transition temperature  $T_c$  and the critical current density  $J_c$  of the samples were measured using both a standard four-probes and an inductive method. The latter is done by measuring the third harmonic component voltage across a small sensor coil mounted very close to the film surface, as a function of temperature and driving current [15]. Inductive measurements yield as typical values  $T_c = 104$  K,  $\Delta T_c = 4$  K and  $J_c = 0.5$  MA/cm<sup>2</sup>, with minimum spread between samples with correct composition. Four probes resistive measurements on patterned films showed that the etching process did not affect the values of  $T_c$  and  $J_c$ .

## Microwave response

The microwave properties were studied using two different and in many aspects complementary methods: a microwave copper cavity (87 GHz) and a microstrip resonator (1.5 GHz). The former is a high sensitive technique for measurements on unpatterned samples of both the surface resistance and changes of the penetration depth, even in the normal state. The excited mode is here a TE-mode, with  $H$  parallel to the film surface. Conversely, the microstrip resonator is useful to characterise the r.f. power behaviour of patterned films in view of applications. In this geometry, the propagating wave is a TEM-mode, with  $E$  and  $H$  perpendicular to the film surface. Details of each measurement procedure and a comparison between the two techniques have been reported elsewhere [16–18].

The surface resistance  $R_s$  and the changes of the penetration depth  $\lambda$  of the sample under test can be extracted from the quality factor  $Q$  and from the resonance frequency  $f_0$ , which are easily obtained from the measurement of the microwave transmitted power *versus* frequency in each resonant structure. For the TE-mode, the measured (effective) values  $R_{s,\text{eff}}$  and  $\lambda_{\text{eff}}$  of the surface resistance and penetration depth respectively are related to the intrinsic values by [19]:

$$R_{s,\text{eff}} = R_s \left( \coth \frac{t}{\lambda} + \frac{t/\lambda}{\sinh^2(t/\lambda)} \right) \quad (1a)$$

$$\lambda_{\text{eff}} = \lambda \coth(t/\lambda). \quad (1b)$$

The penetration depth data obtained through the cavity measurement have been roughly estimated using the usual two fluid relation in the London clean limit:  $\lambda_L(T) = \lambda_L(0)/[1 - (T/T_c)^4]^{0.5}$ . Using a critical temperature  $T_c = 104$  K, in agreement with inductive measurements, a value  $\lambda_L(0)$  of about 400 nm is obtained. This estimate is compatible with previous results [20], even if indicative of screening properties somehow influenced by the granular properties of the film, as it will be shown later on. In Figure 3 the quantity  $[\lambda(0)/\lambda(T)]^2$  is plotted as a function of the reduced temperature  $t = T/T_c$ . In the inset, the low temperature region is magnified to show an almost linear dependence at the lowest  $T$ . The linear slope  $\Delta\lambda/\Delta T$  is about 1.2 nm K<sup>-1</sup>, much higher than corresponding slopes reported for  $\text{YBa}_2\text{Cu}_3\text{O}_{7-\delta}$  single

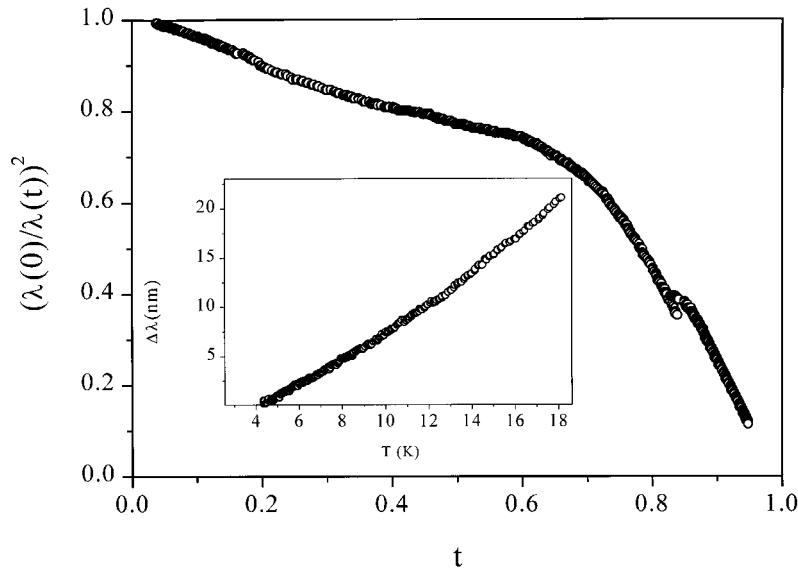


**Fig. 3.**  $[\lambda(0)/\lambda(t)]^2$  as a function of reduced temperature  $t = T/T_c$  measured at 87 GHz. In the inset the quantity  $\Delta\lambda(T) = \lambda(T) - \lambda(4 \text{ K})$  is plotted in the temperature region  $T < 20 \text{ K}$ .

crystals [6] but in good agreement with previous results on  $\text{Tl}_2\text{Ba}_2\text{CuO}_{6+\delta}$  and  $\text{Bi}_2\text{Sr}_2\text{CaCu}_2\text{O}_8$  single crystals [21]. In the framework of the  $d$ -wave theory ( $d_{x^2-y^2}$  state with a cylindrical Fermi surface), for a clean superconductor the measured slope at low temperature is inversely proportional to the gap maximum  $\Delta_0$  over the Fermi surface [22]:  $\Delta\lambda/\Delta T \approx \ln 2(\lambda(0)/\Delta_0)$ . From the value found ( $\Delta_0 \approx 19 \text{ meV}$ ) one yields a ratio  $\Delta_0/T_c \sim 2.3$ , consistent with theory.

As for the surface resistance, the minimum  $R_s$  values obtained at 4.2 K with the microstrip method and the copper cavity are  $60 \mu\Omega$  at 1.5 GHz and  $6 \text{ m}\Omega$  at 87 GHz, respectively. At 77 K the cavity data, if scaled with the usual quadratic frequency law, are not far from the results presented by Willemsen *et al.* [20] ( $R_{s,\text{min}} \sim 50 \mu\Omega$  at 3.7 GHz) on unpatterned samples. On the contrary, the microstrip data are affected by a higher residual term, which therefore doesn't follow the expected  $\omega^2$  dependence. Since radiation losses in the microstrip have been estimated to be of the order of  $1 \mu\Omega$  [17], in our opinion this discrepancy may be related to an enhancement of losses at film edges, which are fairly degraded by patterning. Due to the crowding of current, in fact, the contribution of these regions to the overall conducting losses can be large and completely driven by weak links.

In Figure 4 the effective surface resistance  $R_{s,\text{eff}}$  as a function of temperature is plotted for one of the samples measured in the copper cavity. It is worth noting that at 90 K Tl-2212 samples still showed  $R_s$  values below  $1 \text{ m}\Omega$ . As magnified in the inset, a linear temperature dependence is displayed in the low temperature region. Within the two fluid model, this behavior is consistent with the linear law observed in the penetration depth data.

In Figure 5 the surface resistance measured at 1.5 GHz and at different temperatures as a function of the peak current density  $J_{\text{peak}}$  induced in the microstrip resonator

is shown.  $J_{\text{peak}}$  is given by [23]:

$$J_{\text{peak}} \approx \frac{3I}{2\pi wt} \sqrt{\frac{w}{\lambda}} \quad (2)$$

where  $w$  is the microstrip width and  $t$  is the film thickness.  $I$  (mA) is the total current circulating in the meanderline and is related to the microwave input power  $P_{\text{in}}$  (mW) through the relation [24]:

$$I = \sqrt{\frac{4QP_{\text{in}}S_{12}}{\pi Z_0}} \quad (3)$$

where  $Q$  is the unloaded quality factor,  $S_{12}$  is the transmission scattering parameter, and  $Z_0$  is the intrinsic impedance of the transmission line. The maximum current density corresponds to a microwave input power of 10 mW. For temperatures between 4 and 50 K, the surface resistance shows a rapid increase at low input power levels followed by a quite flat dependence. This is likely due to flux penetration between grains as soon as r.f. magnetic field exceeds some reduced critical field value, associated to the properties of the weak links. In this temperature range  $R_s$  values are more than one order of magnitude lower than copper up to the maximum power available.

The nonlinear losses of the samples have been also characterized by introducing the dimensionless parameter  $r = \Delta R_s / \Delta X_s = \Delta(1/Q) / (-2\Delta f/f)$  [25,26], which is independent of the resonator geometry and can be easily determined from the experimental data. Observing the change of both  $Q$  and  $f_0$  as a function of the input power feeding the resonator, we found  $r \approx 1$  at  $T = 10 \text{ K}$ . This is consistent with the idea that dissipation induced by normal zones or by grain boundaries is the dominant loss mechanism in the microstrip [25].

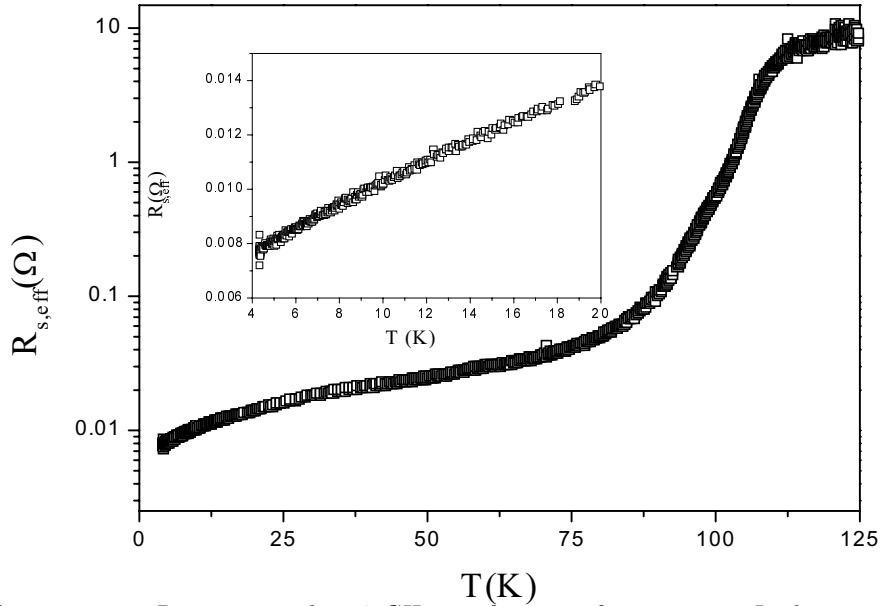


**Fig. 4.** Effective surface resistance  $R_{s,\text{eff}}$  measured at 87 GHz as a function of temperature. In the inset the temperature region  $T < 20$  K is magnified.

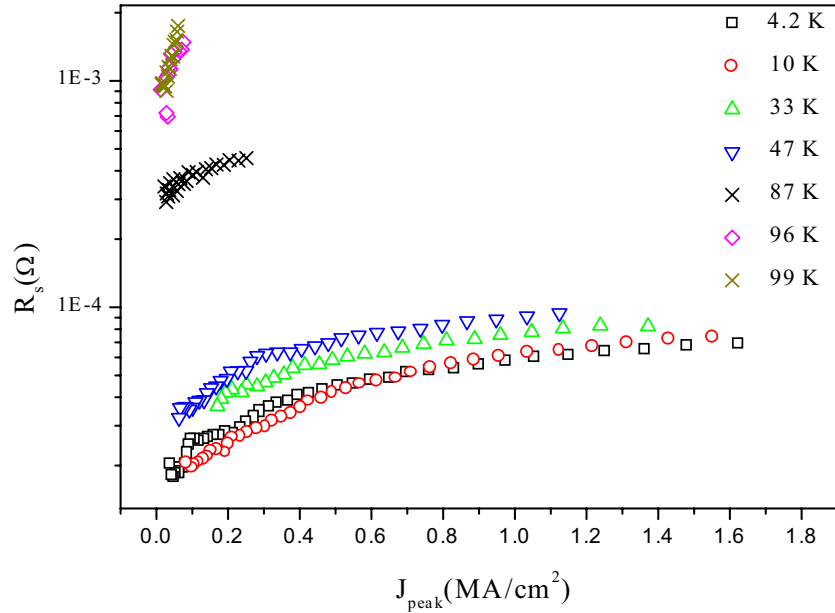


**Fig. 5.** Surface resistance  $R_s$  versus the peak induced current density  $J_{\text{peak}}$  at different temperatures measured at 1.5 GHz using a microstrip resonator.

## Two fluid description

Due to the local and clean nature of HTS, the microwave data can be directly related to the complex conductivity ( $\sigma = \sigma_1 - i\sigma_2$ ) of the superconductor [27]. The relations between  $Z_s$  and  $\sigma$ , at frequencies of our interest and for a reduced temperature  $t = T/T_c < 0.9$  (so that  $\sigma_1 \ll \sigma_2$ ), are:

$$R_s = \sqrt{\frac{\mu_0 \omega}{\sigma_2}} \frac{1}{2} \frac{\sigma_1}{\sigma_2} \quad (4a)$$

$$X_s = \sqrt{\frac{\mu_0 \omega}{\sigma_2}} \quad (4b)$$

It is usual to interpret the complex conductivity in terms of the two fluid model partitioning the conduction electron density  $n$  in the normal and superfluid fractions  $f_n$  and  $f_s$  respectively, with the assumption that  $f_n(t) + f_s(t) = 1$ .

In order to account for a finite residual surface resistance  $R_{\text{res}}$ , a small fraction  $\varepsilon$  of inherently unpaired quasi-particles can be introduced. The previous assumption is correspondingly replaced by the more general approach  $f_n(t) + f_s(t) + \varepsilon = 1$ ,  $0 < \varepsilon \ll 1$ . Data taken from the cavity measurements show values of  $\varepsilon$  ranging between 0.03 and 0.1 [28].

In this framework the conductivity can be written as:

$$\sigma_s(t) = \sigma_1(t) - i\sigma_2(t) = \frac{ne^2}{m^*} \left[ \frac{f_n(t) + \varepsilon}{1/\tau(t) + i\omega} + \frac{f_s(t)}{i\omega} \right] \quad (5)$$

where  $n$  is the quasiparticle density at the Fermi level,  $e$  the electronic unit charge,  $m^*$  and  $\tau$  the effective mass and the scattering time of the quasiparticles respectively.

It is straightforward to see that equation (5) allows to get information on the temperature dependence of  $\tau$  from the real and imaginary parts of conductivity, using the expression:

$$\omega\tau(T) = \frac{\sigma_1(T)}{\sigma_2(0) - \sigma_2(T)}. \quad (6)$$

Here  $\sigma_1$  and  $\sigma_2$  are in turn extracted from the measured value of  $R_s$  and  $X_s$  through equations (4).

As far as HTS are concerned, the inverse of relaxation time  $1/\tau$  has been experimentally observed to have a fast drop just below  $T_c$ , rapidly approaching a value more than two orders of magnitude lower compared to the normal state [8], in striking contrast to the linear behavior above  $T_c$  inferred from the measured d.c. resistivity.

Rather, in the past years different mechanisms have been considered, based on magnetic pair interactions, and strong quasiparticle correlations [6, 16, 29, 30].

Measurements on thin films performed by cavity methods suffer for the indetermination on the value of  $\lambda(0)$  and for the finite thickness of the samples, which can give relevant correction at temperatures close to  $T_c$ . In this context, it is sometimes convenient to introduce the adimensional quantity:

$$R = \frac{T}{R_s} \frac{\partial X_s}{\partial T} \quad (7)$$

$R$  can be easily determined by the experimental data. Neglecting relaxation effects ( $\omega\tau \ll 1$ ), this quantity can be written within a two fluid model as:

$$R = \frac{T(\partial f_n / \partial T)}{(f_n + \varepsilon)} \frac{1}{\omega\tau}. \quad (8)$$

It can be easily shown using equation (5) that  $R$  is thickness independent. Furthermore, in the vicinity of the transition temperature the temperature dependence of the normal fluid component  $f_n$  can be approximated by a power law  $f_n = f[(T/T_c)^m]$ , and  $\varepsilon \ll f_n$ , so that using equation (8)  $R$  can be directly related to the scattering time through the relation:  $R \approx m/\omega\tau$ . However, even in case of more complicate temperature dependence of the quasiparticle density  $f_n(T)$ , its contribution to  $R(T)$  is quite moderate. For example, assuming the empirical relation  $f_n = 3t/7 + 4t^6/7$ , sometimes used to describe the experimental results of high quality YBCO single crystals [31], it is in the overall temperature range:  $1 \leq T(\partial f_n / \partial T) / f_n \leq 3$ .

The  $R$  factor extracted from the copper cavity data is plotted in Figure 6 as a function of temperature and compared with the result obtained using the same technique

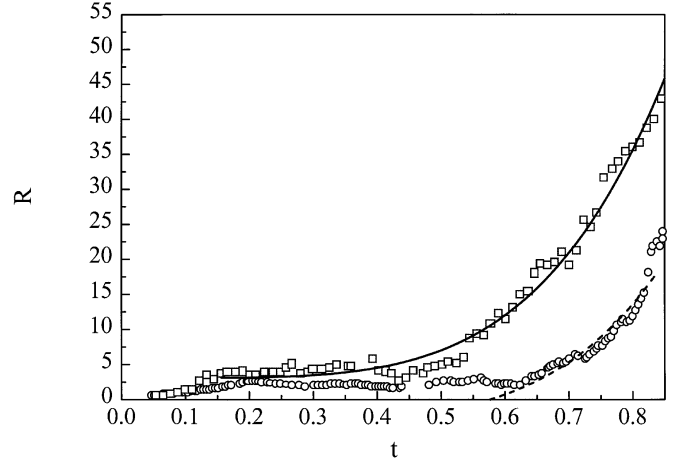


**Fig. 6.**  $R$  as a function of temperature evaluated at 87 GHz for a Tl-2212 film (squares) and the YBCO film (circles) reported in reference [16] (sample A). The continuous and the dashed lines represent the fit performed on YBCO and Tl-2122 films respectively (see text).

on data taken from literature on a high quality epitaxial YBCO film (Ref. [16], sample A). The two set of data show a similar behavior.

As far as YBCO is concerned, for  $t < 0.1$  the quantity  $R$  linearly increases with temperature likely due to the term  $t/\varepsilon$ , which cannot be neglected at the lowest temperatures. For  $0.1 < t < 0.4$  the temperature dependence appears rather flat, showing a rapid increase only for  $T$  approaching  $T_c$ . In this temperature region it is  $R \approx 5$  which, making the assumption that  $m = 1$ , corresponds to  $1/\tau \approx 2.5 \times 10^{12} \text{ s}^{-1}$ .

As for the Tl-2212 sample shown in Figures 2 and 3, the much higher level of defects limits the temperature range over which change in the quasiparticle-scattering rate can be observed. At the lowest temperatures, the fraction  $\varepsilon$  of unpaired quasiparticles is in fact the dominant contribution to dissipation. At intermediate temperatures, nevertheless, it is  $R \approx 2$  almost constant, yielding a value  $1/\tau \approx 1 \times 10^{12} \text{ s}^{-1}$ .

Using the reference YBCO film, we made also an attempt to fit the data using the empirical law  $R(T) = A + B(T/T_c)^\alpha$ . From 20 to 90 K this yields an exponent  $\alpha = 4.5 \pm 0.2$  (continuous line in Fig. 6), which is close to the exponential behavior of reference [16] and similar to what reported in reference [32]. For the Tl-2212 sample, at temperatures approaching  $T_c$ , the scattering rate is found to have a strong increase too, at least as fast as  $T^5$ . The dashed curve in Figure 6 describes the above mentioned functional relation for  $R(T)$ , fixing  $\alpha = 5$ .

## Conclusions

Tl-2212 superconducting films were grown by a combined MOCVD and thallium vapor diffusion process. The samples are highly  $c$ -axis oriented and monophasic, showing fairly good transport properties.

The microwave response was measured at 87 GHz on unpatterned samples through a copper cavity and at 1.5 GHz on wet etching patterned films by means of a microstrip resonator. While the data from cavity outline that MOCVD is capable of producing samples with a very low surface resistance, comparable with the best results present in literature, it is found that the r.f. properties of Tl-2212 microstrips are mainly dominated by weak links, especially in terms of  $R_{res}$  and power handling capability.

The temperature dependence of the scattering time  $\tau$  was evaluated from the microwave measurements through the adimensional parameter  $R$ , without any assumption on the value of  $\lambda(0)$ . Our data show that  $\tau$  in Tl-2212 films increases at least as  $T^5$ , showing a behavior similar to the one observed in YBCO films.

We wish to thank M. Hein and T. Kaiser for stimulating discussions. We are grateful to S. Hensen for providing the YBCO data of reference [16] in electronic form. The technical support of A. Maggio and S. Marrazzo is also gratefully acknowledged. G. Pica has been partially supported by Fondo Sociale Europeo.

## References

- H. Schneidewind, M. Zeisberger, H. Bruchlos, M. Manzel, T. Kaiser, *Inst. Phys. Conf. Ser.* **167**, 383 (2000).
- M. Zeisberger, M. Manzel, H. Bruchlos, M. Diegel, F. Thrum, M. Klinger, A. Abramowicz, *IEEE Trans. Appl. Supercond.* **9**, 3897 (1999).
- M.M. Eddy, J.Z. Sun, R.D. Hammond, L. Drabeck, I.B. Ferreira, K. Holczer, G. Grüner, *J. Appl. Phys.* **70**, 496 (1991).
- J.D. O'Connor, A.P. Jenkins, D. Dew-Hughes, M.J. Goringe, C.R.M. Grovenor, *IEEE Trans. Appl. Supercond.* **7**, 1899 (1997).
- D.W. Face, F.M. Pellicone, R.J. Small, L.B. Bao, M.S. Warrington, C. Wilker, *IEEE Trans. Appl. Supercond.* **9**, 2492 (1999).
- M.R. Trunin, *J. Supercond.* **11**, 381 (1998).
- D.M. Broun, D.C. Morgan, R.J. Ormeno, S.F. Lee, A.W. Tyler, A.P. Mackenzie, J.R. Waldram, *Physica C* **282-287**, 1467 (1997).
- D.A. Bonn, Ruixing Liang, T.M. Riseman, D.J. Baar, D.C. Morgan, K. Zhang, P. Dosanjh, T.L. Duty, A. MacFarlane, G.D. Morris, J.H. Brewer, W.N. Hardy, C. Kallin, A.J. Berlinsky, *Phys. Rev. B* **47**, 11314 (1993).
- S. Huber, M. Manzel, H. Bruchlos, S. Hensen, G. Müller, *Physica C* **244**, 337 (1995).
- B.A. Willemsen, K.E. Kihlstrom, T. Dahm, *Appl. Phys. Lett.* **74**, 753 (1999).
- G. Malandrino, F. Castelli, I.L. Fragalà, *Inorg. Chim. Acta* **224**, 203 (1994).
- B.T. Ahn, W.Y. Lee, R. Beyers, *Appl. Phys. Lett.* **60**, 2150 (1992).
- J.D. O'Connor, A.P. Jenkins, C.R.M. Grovenor, M.J. Goringe, D. Dew-Hughes, *Supercond. Sci. Technol.* **11**, 207 (1998).
- G. Malandrino, A.M. Borz, I.L. Fragalà, A. Andreone, A. Cassinese, G. Pica (unpublished).
- J.H. Claassen, M.E. Reeves, R.J. Soulen, *Rev. Sci. Instrum.* **62**, 996 (1991).
- S. Hensen, G. Müller, C.T. Rieck, K. Scharnberg, *Phys. Rev. B* **56**, 6237 (1997).
- A. Andreone, A. Cassinese, A. Di Chiara, M. Iavarone, F. Palomba, A. Ruosi, R. Vaglio, *J. Appl. Phys.* **82**, 1736 (1997).
- A. Andreone, C. Aruta, M. Iavarone, F. Palomba, M.L. Russo, M. Salluzzo, R. Vaglio, A. Cassinese, M.A. Hein, T. Kaiser, G. Mueller, M. Perpeet, *Physica C* **319**, 141 (1999).
- N. Klein, H. Chaloupka, G. Müller, S. Orbach, H. Piel, B. Roas, L. Schultz, U. Klein, M. Peiniger, *J. Appl. Phys.* **67**, 6940 (1990).
- B.A. Willemsen, K.E. Kihlstrom, T. Dahm, J. Scalapino, B. Gowe, D.A. Bonn, W.N. Hardy, *Phys. Rev. B* **58**, 6650 (1998).
- D.M. Broun, D.C. Morgan, R.J. Ormeno, S.F. Lee, A.W. Tyler, A.P. Mackenzie, J.R. Waldram, *Phys. Rev. B* **56**, R11443 (1997).
- P.J. Hirschfeld, N. Goldenfeld, *Phys. Rev. B* **48**, 4219 (1993).
- R.B. Hammond, E.R. Soares, B.A. Willemsen, T. Dahm, D.J. Scalapino, J.R. Schrieffer, *J. Appl. Phys.* **84**, 5662 (1998).
- M.J. Lancaster, *Passive Microwave Device Applications of High Temperature Superconductors* (Cambridge University Press, Cambridge, 1997).
- J. Halbritter, *J. Appl. Phys.* **68**, 6315 (1990).
- M.A. Golosovsky, H.J. Snortland, M.R. Beasley, *Phys. Rev. B* **51**, 6462 (1995).
- S.B. Nam, *Phys. Rev.* **156**, 470 (1967); *ibid.*, 487 (1967).
- A. Cassinese, G. Müller, M. Hein, S. Hensen, *Eur. Phys. J. B* **14**, 605 (2000).
- A.A. Golubov, M.R. Trunin, A.A. Zhukov, O.V. Dolgov, S.V. Shulga, *Pis'ma Zh. Exp. Teor. Fiz.* **62**, 477 (1995) [*JETP Lett.* **62**, 496 (1995)].
- T. Jacobs, K. Numssen, R. Schwab, R. Heidinger, J. Halbritter, *IEEE Trans. Appl. Supercond.* **7**, 1917 (1997).
- H.J. Fink, *Phys. Rev. B* **58**, 9415 (1998).
- A. Hosseini, R. Harri, S. Kamal, P. Dosanjh, J. Preston, R. Liang, W.N. Hardy, D.A. Bonn, *Phys. Rev. B* **60**, 1349 (1999).